ORGANOMETALLICS

Article

pubs.acs.org/Organometallics

Effects of Hindrance in N-Pyridyl Imidazolylidenes Coordinated to Iridium on Structure and Catalysis

Zephen G. Specht,[†] Douglas B. Grotjahn,*[,†] Curtis E. Moore,[‡] and Arnold L. Rheingold[‡]

[†]Department of Chemistry and Biochemistry, San Diego State University, 5500 Campanile Drive, San Diego, California 92182-1030, United States

[‡]Department of Chemistry and Biochemistry, University of California at San Diego, La Jolla, California 92093-0358, United States

Supporting Information

ABSTRACT: The unhindered *N*-pyrid-2-yl imidazolidene NHC ligand has been shown to chelate to a Cp*Ir fragment (**1**). With the goal of weakening the coordination of the pyridyl substituent and enabling its role as pendant base or hemilabile ligand, a *tert*-butyl group at C-6 next to the pyridyl N was installed. Attempted coordination of the newly synthesized carbene ligand avoided N-coordination entirely, but led to unexpected C-metalation at C-3 by the Cp*Ir center. Successful formation of a weakly N-coordinated analogue was achieved by synthesizing a ligand with a second *tert*-butyl group at C-4. The complexes were studied using X-ray crystallography and NMR spectroscopy. The X-ray crystal structure of di-*tert*-butyl analogue **6** showed that in the solid the complex existed as a chloride-bridged dimer, with the pyridyl nitrogen uncoordinated. In solution, ^{15}N chemical shift information revealed that **6** existed with the pyridyl substituent N-coordinated, presumably as a monomer, but that addition of an amine ligand readily opened the chelate. Finally, **6** was used as a catalyst for intramolecular hydroamination of primary and secondary alkenylamines. Comparing (heteroaryl)NHC species, each with a *tert*-butyl group next to the nitrogen, which enables hydroamination, the rate differences are very modest but increase in the order imidazolyl < pyridyl < pyrimidyl, which may be an effect of basicity but because of the similarity in rates is better ascribed to counterbalancing of more than one factor, including hemilability. The (4,6-di-*tert*-butyl)pyridyl species **6** was shown to be much more effective compared to parent compound **1** without the *tert*-butyl groups, in which the chelating group was more tightly bound.

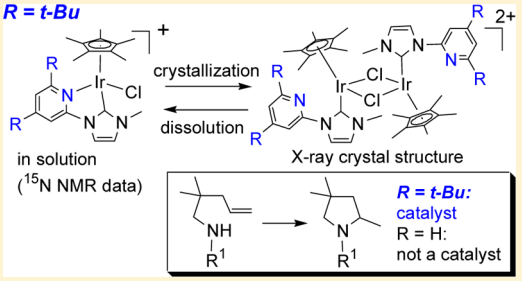

INTRODUCTION

N-Heterocyclic carbene (NHC) complexes have been shown to be extremely versatile and stable catalysts for a wide range of reactions such as olefin metathesis, transfer hydrogenation, and C−C coupling reactions.[1−3] These NHCs are attractive ligands due to their relative air, moisture, and thermal stability[4−6] because of their strong σ-donating ability and poor back-bonding of their complexes.[7−11]

In 2011 our group reported a series of iridium-based NHC ligands that feature a potential pendant base as a substituent.[12] Several of the examples (including **4**, Chart 1) featured a pyrimidine nitrogen, with one example of an imidazolyl nitrogen (**2**), bound to the iridium metal. The Ir−N bond was shown through variable-temperature NMR studies and X-ray crystallography to weaken significantly as more steric bulk was added around the nitrogen atoms on the pyrimidine ring. The most reactive complex (**4**) featured a *tert*-butyl group next to each heteroaryl nitrogen atom and was able to perform intramolecular hydroamination of alkenes by primary and secondary amine groups. In summary, controlling ligand sterics near the nitrogen−iridium bond lowered the energy required to break the bond and increased catalytic activity.

Although our study conclusively demonstrated that greater catalyst activity resulted from increased steric bulk on (pyrimidyl)NHC complexes, it was less clear what role was played by basicity of the heteroaryl group. (Imidazolyl)NHC species **2** was somewhat less active than **4**, but this could be due to increased pendant basicity or because of altered ligand−metal bond strength because of different geometry imposed by the five-membered imidazole ring. Therefore, we decided to study pyridyl analogues of pyrimidyl species **4** because the ring size would be constant. Because protonated pyrimidine and pyridine are of different basicity (pK_a = 1.3 and 5.2, respectively),[13,14] in complexes such as **4**−**6**, the related pendant bases could be expected to have very different coordination and catalytic properties.

(Pyridyl)NHC complex **1** was made in 2008[15] and would be expected to have a very strong Ir−N bond, as we determined to be the case for unhindered pyrimidine analogue **3**.[16] Structures **5** and **6** (Chart 1) show the desired pyridine-based compounds targeted in the study reported here. Although a few iridium (pyridyl)NHC ligand catalysts have been reported in recent years,[15,17−19] as far as we are aware, none of these feature sterically hindered pendant pyridines such as the ones reported here.

Received: July 30, 2013
Published: October 14, 2013

dx.doi.org/10.1021/om400758b | *Organometallics* 2013, 32, 6400−6409

Chart 1. Cp*Ir Complexes Considered in This Study Including Published Species 1,[15] 2,[12] 3,[16] and 4[12]

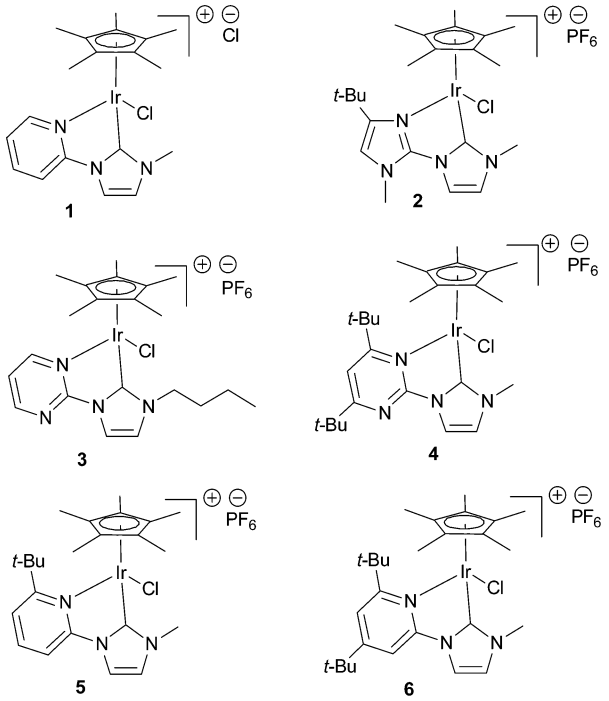

RESULTS AND DISCUSSION

Synthesis. As mentioned in the Introduction, in order to change the basicity of the substituent in pyrimidyl NHC systems without changing chelate geometry, pyridyl NHCs were attractive targets. We embarked on the synthesis of **5**, Chart 1. Starting material **7** was subjected to addition−elimination using the sodium salt of imidazole, producing **8** in high yield. Subsequent N-methylation of the more nucleophilic and less hindered imidazole ring proceeded without incident, giving **9**, and after anion exchange, **10**. However, as described below, due to unexpected metalation of the pyridine ring at a ring carbon, producing **22**, inclusion of a second *tert*-butyl group as in **6** was proposed to suppress metalation.

In order to create the di-*tert*-butyl pyridyl imidazolium salt **19**, and thus form compound **6**, first alkynyl ketone **12** was created using a method published by Grotjahn et al.[20] Streitwieser's published method was used to make pyrancarboxylate **13**.[21] The oxygen in the ring was then exchanged for a nitrogen atom using ammonia, and then the methyl ester group was removed by hydrolysis and decarboxylation using strong acid and heat to give **15**. Phosphorus pentachloride chlorinated **15** to form **16** in good yield, after which a copper-catalyzed displacement reaction was used to form **17**. It should be noted here that the methods used to form compound **8** were first used to try to create **17**. However, the reaction failed to go to completion, even at higher temperatures and longer reaction times. The final steps of precursor synthesis followed the previously listed methods for methylation and anion exchange, converting **17** into **18** and then **19**. The salts were characterized by elemental analysis and NMR spectroscopy, where the ^{1}H NMR spectra showed a very low field resonance in the range δ 9.28−11.62 ppm, characteristic of the NC*H*N imidazolium proton.

Air-stable ionic (bis-NHC)silver hexafluorophosphate complexes were prepared in yields above 95% following the method reported by Wang and Lin,[22] except that no added phase transfer agent was needed. Lack of added quaternary ammonium salt simplified isolation to partitioning the mixture between water and CH_2Cl_2 in a separatory funnel. Transformations of the imidazolium salts to their corresponding

Scheme 1. Syntheses of Ligands

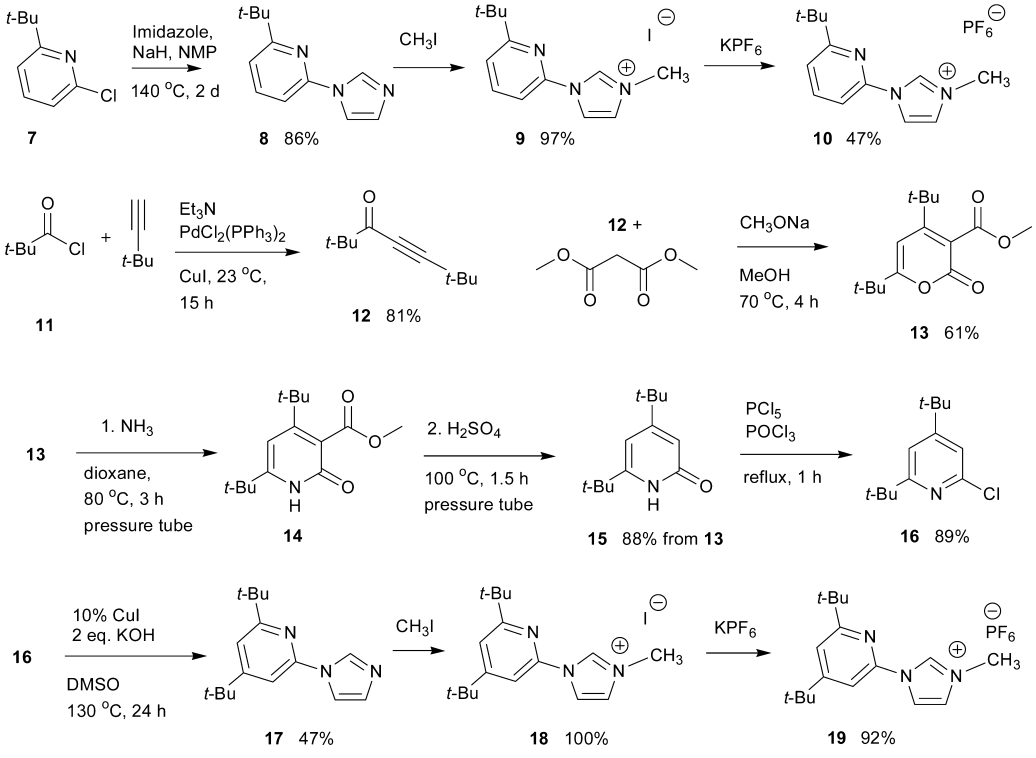

dx.doi.org/10.1021/om400758b | *Organometallics* 2013, 32, 6400−6409

Scheme 2. Syntheses of Silver and Iridium Complexes and Monomer−Dimer Equilibrium of 6

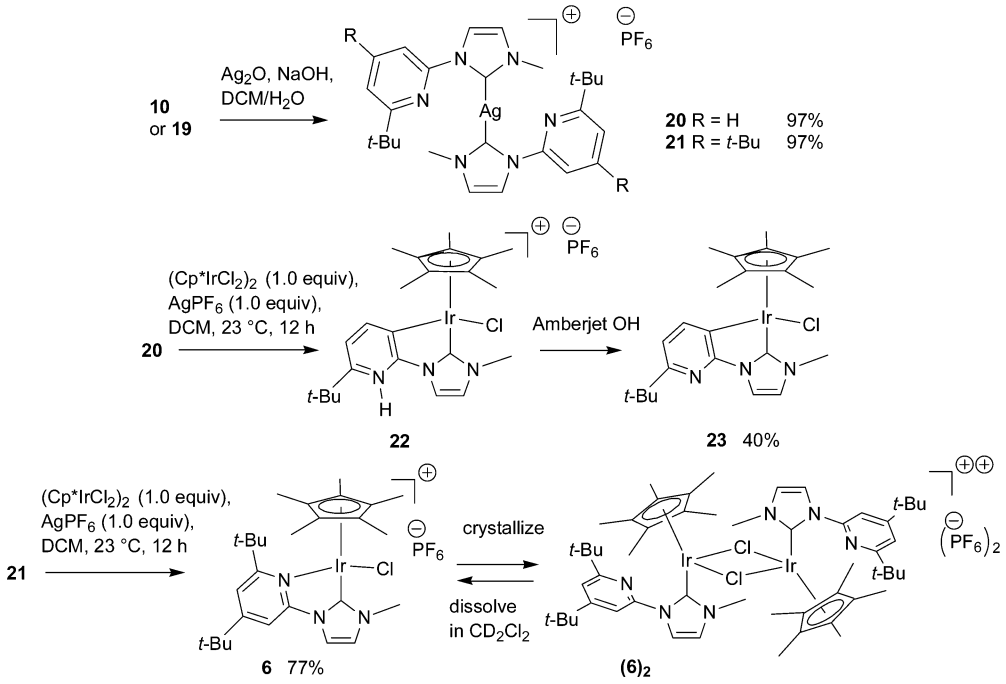

silver-NHC complexes led to downfield shifts of the C-2 carbon from 133.8 ppm to 135.0 ppm to 181.2 ppm, respectively. The ^{13}C NMR signal for the carbene carbon attached to silver appeared as two doublets, for example in the case of **21**, at δ 181.2 ppm, with $^{1}J_{C-Ag-109}$ = 214.9 Hz and $^{1}J_{C-Ag-107}$ = 185.7 Hz, as noted by Arduengo et al.[23] and subsequently others.[22,24,25] The isolated silver compounds were air stable, and only a small amount of degradation was seen in a vial filled with air in a closed drawer after months.

Graphical summaries of 2D NMR data and assignments of all proton and carbon resonances for compounds **6**, **9**, **10**, **14**−**17**, **19**−**21**, and **23** are given in the Supporting Information.

The isolated Ag complexes were used for transmetalation by $[Cp^*Ir(\mu\text{-}Cl)Cl]_2$ and sufficient $AgPF_6$. The mixtures were stirred for 12−18 h and then filtered through Celite, followed by concentration under vacuum. In the case of attempted synthesis of compound **5**, analysis of the product mixture after workup by ^{1}H NMR spectroscopy suggested that only two mutually coupled protons were left on the pyridyl ring, as evidenced by two sharp doublets at 8.54 and 7.26 ppm (J = 7.6 Hz). A downfield broad one-proton signal was seen near 12.6 ppm, suggesting the presence of an NH and the formation of **22** rather than **5**. In confirmation of this alternative structure, addition of base allowed the isolation of neutral species **23** by crystallization of the crude mixture as a red-orange solid in moderate yield.

Efforts were made to see if target complex **5** was formed at early stages during the synthesis, which ultimately led to **22** and **23**. An NMR tube reaction conducted in CD_2Cl_2 by mixing **20**, $[Cp^*Ir(\mu\text{-}Cl)Cl]_2$, and $AgPF_6$ showed a somewhat complicated mixture, with evidence even in the first hour of reaction of a downfield NH proton resonance associated with **22**. Our conclusion was that simple changes in reaction conditions alone would not allow one to make **5**, because of fast, competitive metalation at carbon of the pyridyl ring. Cyclometalations by Cp*Ir fragments are well known; for one example, see Li et al.[26]

X-ray Diffraction and Raman and NMR Spectroscopic Analysis of 6 and 23 and Related Species. Full comparison of the structure of **6** in the solid state and solution gave interesting results, as described here. The crystal structures for both **6** and **23** were obtained, with the crystallographic data listed in Table S1. The molecular structures are shown in Figures 1 and 2 for compounds **23** and **6**, respectively. Figure 1

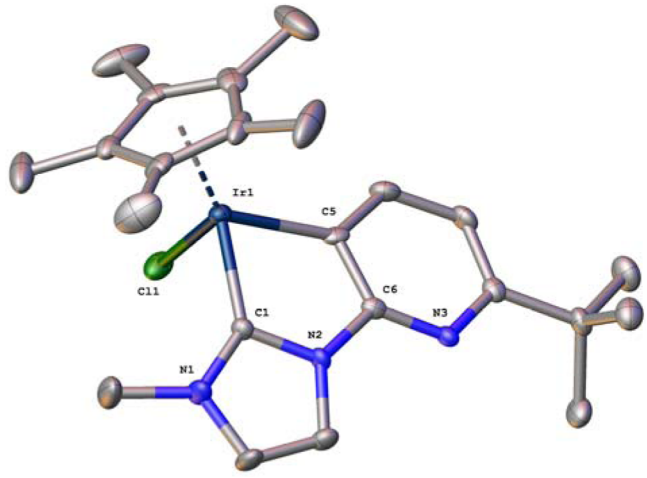

Figure 1. ORTEP diagram of **23**, confirming metalation of the pyridyl substituent at carbon.

shows that the mono-*tert*-butyl pyridine ring metalated at the C3 carbon (labeled C5 in Figure 1), forming unexpected product **23**, as previously shown in Scheme 2. Metalation at carbon can be prevented by steric hindrance of the di-*tert*-butyl pyridine ring.

Interestingly, the X-ray crystallographic data for **6** (Figure 2) revealed that in the crystalline state the compound is dimer $(\mathbf{6})_2$, forming through bridging chlorides, rather than the expected monomer with a chelate and an Ir−N bond.

dx.doi.org/10.1021/om400758b | *Organometallics* 2013, 32, 6400−6409

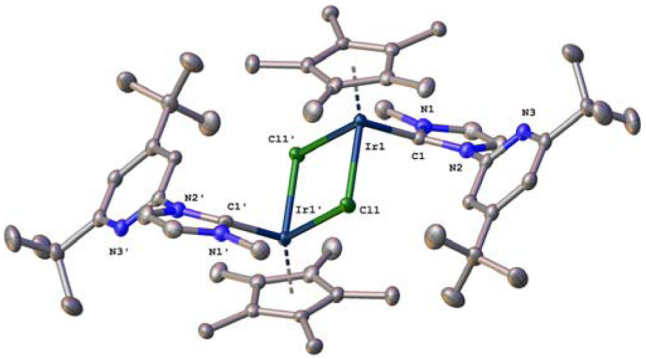

Figure 2. ORTEP diagram of the (di-*tert*-butylpyridyl)NHC complex as dimer $(\mathbf{6})_2$ with bridging chloride ligands and an intact, unmetalated ligand.

Comparing the Ir−C or Ir−N bond distances of the pyrimidine compounds **3** and **4** to that of the pyridine-based compounds **5** and **6** is not possible due to the fact that **23** rather than **5** formed and that dimer $(\mathbf{6})_2$ formed in the solid state rather than the chelating monomer. Apparently the Ir−Cl bridging interaction and the Ir−N interactions must have relatively similar strengths and can be reversibly formed, supporting the notion of Ir−N bonds weakened by steric destabilization.

To begin to study the relationship of **6** and dimer $(\mathbf{6})_2$, attempts were made to identity the bridging chloride dimer using Raman spectra of solid samples (spectra shown in the Supporting Information). Complex **23** showed a terminal Ir−Cl stretch at 280.2 cm^{-1}, and **1**-PF_6 also with a terminal Ir−Cl bond showed a single stretch at 282.8 cm^{-1}. In our hands, the dimer $[Cp^*Ir(\mu\text{-}Cl)Cl]_2$ also showed a peak at 280.3 (terminal Ir−Cl), but also a stretch at 254.9 cm^{-1}, previously assigned as due to the bridging Cl.[27−30] The spectrum of **6** showed a peak at 289.8 cm^{-1}, and no peak between there and 177.2 cm^{-1}.

More direct and conclusive evidence for the bonding of the heteroaryl substituent was sought, particularly in the solution phase, where catalysis would occur. Appreciable ^{15}N chemical shift changes accompanying coordination, hydrogen bonding, or protonation of a sp^2-hybridized heteroaryl nitrogen have previously given us a uniquely diagnostic tool for determining bonding changes of bifunctional catalysts,[31−34] and the work here is no exception. In order to study how **6** behaves in solution, ^{15}N chemical shift data were gathered by $^1H-^{15}N$ HMBC spectra (Table 1) on unlabeled compound **6** and the product of benzylamine binding, **6-BA** (Scheme 3), as we had done previously for species **2** and **4** and their benzylamine adducts also shown in Scheme 3.[12]

In addition to looking at **6** and **6-BA**, to provide models for the ^{15}N chemical shift in the absence of coordination, synthetic precursors **19** and **21** were also examined (Table 1, entries 11 to 14). One can see from entries 11 and 12 that chemical changes remote from a pendant heteroaryl nitrogen, such as conversion of an imidazolium salt to its corresponding silver-NHC complex, do not lead to appreciable chemical shift changes (no more than 5 ppm) for the pendant heteroaryl nitrogen. The same conclusion is reached when looking at data for three different heteroaryl groups (di-*tert*-butylpyridyl, its

Table 1. ^{15}N NMR Chemical Shift Data for Complexes and Model Compounds[a]

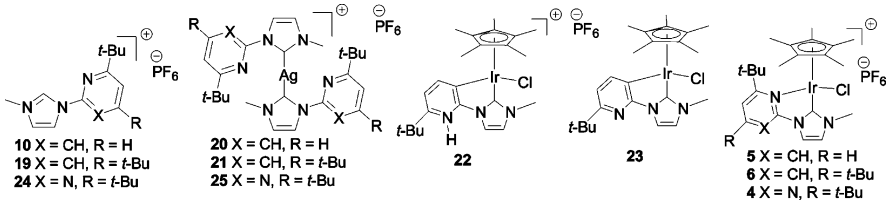

					^{15}N NMR chemical shifts				
					heteroaryl		imidazolium or imidazolylidene		
entry	heteroaryl group	compound	solvent	temp (°C)	N free	N interacting	N1 (N-Me)	N-3 (with heteroaryl)	coordinated $PhCH_2NH_2$
1[b]	imidazole	**2**[b]	acetone-d_6	30	−239.2	−224.4 (coord)	−203.0	−193.7	
2[b]		**2-BA**	CD_2Cl_2	−90	−226.8	−135.3 (H-bond)	−189.8	−195.9	−385.2
3[b]	pyrimidine	**24**	CD_2Cl_2	30	−125.7		−204.1	−182.3	
4[b]	X = N, R = *t*-Bu	**25**	CD_2Cl_2	30	−125.4		−195.4	−171.2	
5[b]		**4**	acetone-d_6	−18	−128.6	−191.2 (coord)	−201.8	−177.7	
6[b]		**4-BA**	CD_2Cl_2	−90	−100.6	−118.0 (H-bond)	−192.4	−170.0	−388.4[c]
7	pyridine	**1-PF_6**[d]	CD_3CN	30		−176.9 (coord)	−203.1	−178.7	
8	pyridine	**10**	$CDCl_3$	30	−98.5		−205.7	−183.5	
9	X = CH, R = H	**20**	CD_2Cl_2	30	−93.2		−195.7	−171.6	
10		**23**	$CDCl_3$	30	−113.8		−210.0	−164.6	
11	pyridine	**19**	$CDCl_3$	30	−104.5		−205.9	−183.2	
12	X = CH, R = *t*-Bu	**21**	CD_2Cl_2	30	−99.9		−196.0	−171.0	
13		**6**	CD_2Cl_2	−40		−181.4 (coord)	−204.0	−178.8	
14		**6-BA**	CD_2Cl_2	−60		−96.2 (H-bond)	−191.5	−170.4	−385.0[c]

[a]Measured except as otherwise noted for the benzylamine ligand of **4-BA** using $^1H-^{15}N$ gHMBC data. See Supporting Information for assigned cross-peaks. In the "N interacting" column, "coord" means coordinated, "H-bond" means engaged in a hydrogen bond. [b]Data in entries 1 to 6 are from ref 12 for ready comparison with new data. The ^{15}N shifts for **2** given in the reference were found to be mistaken due to errors in calculation and are here corrected. [c]Data for compound made with ^{15}N-labeled benzylamine, from the 1D ^{15}N spectrum instead of $^1H-^{15}N$ gHMBC, probe temperature 30 °C. [d]Analogue of **1** with PF_6^- instead of chloride counterion.

dx.doi.org/10.1021/om400758b | *Organometallics* 2013, 32, 6400−6409

Scheme 3. ^{15}N NMR Comparison between Products of Reacting 2, 4, and 6 with Benzylamine[a]

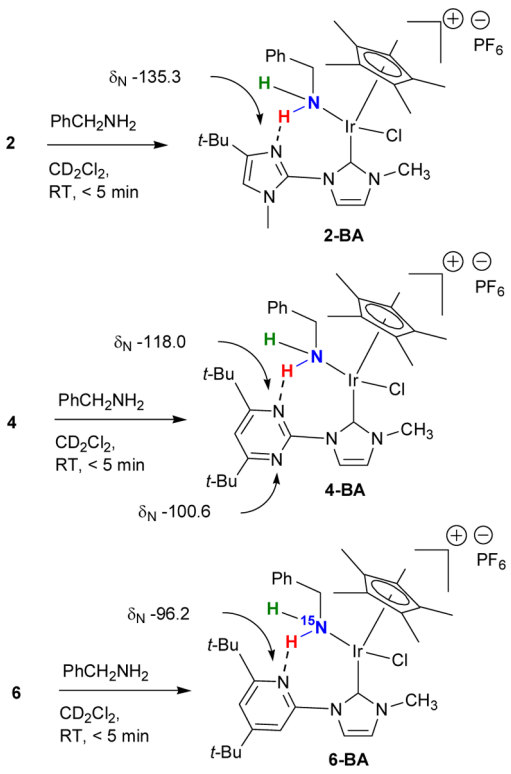

[a]Data for **2-BA** and **4-BA** are from ref 12.

mono *tert*-butyl analogue, as well as for the di-*tert*-butylpyrimidyl system previously reported[12]) (entries 11 and 12; 8 and 9; and 3 and 4). Turning to the specific case of the di-*tert*-butylpyridine substituent relevant to **6**, the ^{15}N shifts showed that as an imidazolium salt with no coordination to the pyridine ring the shift is −104.5 ppm (entry 11). Significantly, the ^{15}N pyridine peak for **6** (entry 13) shifts upfield by 76.9 ppm to −181.4 ppm, definitely indicating coordination to the metal.[31,33] *The NMR evidence strongly implicates formulation of* **6** *as the chelate shown, in methylene chloride.* Similarly, for pyrimidyl system **4**, with one coordinating N and one free N, a chemical shift difference of 62.6 ppm was noted (Table 1, entry 5).

1D ^{1}H and ^{13}C{^{1}H} NMR spectra for **6** in methylene chloride solution showed a single set of peaks, whether at +30 °C or at −40 °C, and although there was some slight broadening of some of the resonances, the appearance of the peaks did not change over the temperature range mentioned. The estimated detection limit for any minor species may be conservatively estimated as 5%. Given the identification of **6** as the chelate in CD_2Cl_2 at −40 °C (by ^{15}N chemical shift data, with the −18 °C temperature used to sharpen signals and allow for detection of cross-peaks) and the appearance of one set of NMR peaks or ^{1}H−^{13}C cross-peaks over a temperature range of 70 °C, we conclude that if chloride-bridged dimer $(\mathbf{6})_2$ is also present, it must be in small amounts. However, our proposal is that when the mixture is subjected to conditions where crystals slowly form, the chloride-bridged dimer $(\mathbf{6})_2$ can form because the dicationic salt form is presumably less soluble under the conditions of crystallization.

In order to investigate the lability of the chelate in **6**, the complex was treated with a primary amine, ^{15}N-labeled benzyl amine. Approximately 0.04 mmol of **6** was combined with an equimolar amount of labeled benzylamine, with 0.6 mL of CD_2Cl_2 as solvent, forming **6-BA** (Scheme 3), which showed a structure similar to that of previously published amine adducts **2-BA** and **4-BA**. ^{15}N NMR data for the three benzylamine adducts are summarized in Table 1.

When the chelate is opened by binding of benzylamine to the iridium, in **6-BA** the pyridine nitrogen signal shifts downfield to −96.2 ppm, which is clear evidence for no more coordination to the metal. However, as to the nature of hydrogen bonding, the ^{15}N chemical shift is less diagnostic than in other systems previously examined (e.g., **4-BA**[12] or various heteroaryl phosphines[31,33]): the value for **6-BA** is about 3 ppm upfield that in the closest model compound, **21**, whereas for **4-BA**, which had two pyrimidyl nitrogens that would be equivalent except for hydrogen bonding to one of them, the ^{15}N chemical shift of the hydrogen-bonding N was seen to be 17.4 ppm upfield of the second, noninteracting nitrogen (Table 1, entry 6).

In order to gain more insight into the hydrogen bonding in **6-BA**, the NMR data for the two protons of the bound amino group were examined. In the spectrum of **6-BA** distinctive features include a four-spin system for the $-CH_2NH_2$ unit, with the two NH protons resonating at 6.65 ppm (dddd, J_{HH} = 4.7, 11.6, 11.7 and J_{HN} = 73.1 Hz) and 4.01 ppm (dddd, J_{HH} = 1.5, 10.9, 11.3, and J_{HN} = 70.7 Hz). Because ^{15}N-labeled benzylamine was used, the two distinct one-bond N−H coupling constants were seen, with that of the downfield proton resonance being larger by 2.4 Hz, consistent with a significant difference in chemical environment for the two N−H bonds, one of which is proposed to be engaged in hydrogen bonding.

Intramolecular Hydroamination and Cyclization of Alkenylamines. Catalyzed cyclization of the primary amine **26a** to give **27a** in Scheme 4 was performed in order to compare the (pyridyl)NHC-based catalysts to the previously published pyrimidyl analogues. The reactions were performed in sealed J. Young NMR tubes in order to eliminate any loss of reactant material or accidental introduction of contamination that might be introduced because of sampling, and THF-d_8 was used rather than toluene because it effectively dissolved the catalyst. Table 2 shows that **4** and **6** are very similar in activity.

Scheme 4. Products from Reaction of Primary Amine 26a or Secondary Amine 26b: Cyclization (27a,b), Alkene isomerization (28a,b), and Subsequent Dehydrogenation of 27a (29)

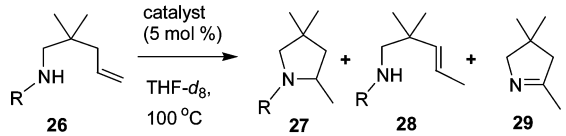

Looking at results from primary amine **26a**, among (pyridyl)NHC derivatives, an increase in conversion occurs on going from **1**, which is virtually inactive, to $[Cp^*Ir(\mu\text{-}Cl)Cl]_2$, and finally to **4** and **6**, which are the most active, but similar to each other in activity. It is interesting to note that the isomerization of **26a** to **28a** occurred only in an appreciable amount using $[Cp^*Ir(\mu\text{-}Cl)Cl]_2$ and in a very small amount using **1**. Using **4** or **6**, the cyclization reaction is essentially

dx.doi.org/10.1021/om400758b | *Organometallics* 2013, 32, 6400−6409

Table 2. Percent Yields for the Cyclization of Primary Amine 26a[a]

	1 h				24 h				72 h			
catalyst	26a	27a	28a	29	26a	27a	28a	29	26a	27a	28a	29
$[Cp^*Ir(\mu\text{-}Cl)Cl]_2$	69	0	17	0	61	1.6	26	0	51	3.6	31	0
1	96	0	2.1	0	92	0	5.6	0	78	0.5	5.6	0
2					65	27	0	0	36	55	3	0
6	68	22	1.1	7.8	0	78	2.0	17	0	72	0.5	26
4	60	31	4.1	9.1	0	78	3.3	21	0	64	0.4	33

[a]**26a** (0.125 mmol) and catalyst (5 mol %; 2.5 mol % in the case of $[Cp^*Ir(\mu\text{-}Cl)Cl]_2$ in THF-d_8 (0.5 mL) at 100 °C). Yields shown are based on ^{1}H NMR spectroscopic analysis, averaging results from two separate runs, except for **4**, using 1,3,5-trimethoxybenzene as an internal standard. Estimated experimental uncertainties in yields are about 2% for larger values and as low as 0.5% for smaller values; hence yield totals may be as much as 105% in some cases, within the uncertainties of the method.

Table 3. Percent Yields for the Cyclization of Secondary Amine 26b[a]

	1 h			24 h			72 h		
catalyst	26b	27b	28b	26b	27b	28b	26b	27b	28b
1	99	0	0	95	1.3	1.0	85	2.6	1.0
6	16	83	0	0	84	0	0	79	0
4	2.9	89	2.0	3.0	89	2.0			
2	37	62	3.9	3.8	86	4.4			

[a]**26b** (0.125 mmol) and catalyst in THF-d_8 (0.5 mL) at 100 °C. Yields shown are based on ^{1}H NMR spectroscopic analysis, averaging results from two separate runs, except for **2** and **4**, using 1,3,5-trimethoxybenzene as an internal standard.

complete within 24 h, but the yield of **27a** (78%) was diminished by a side reaction, dehydrogenation to give imine **29**, the amount of which increased at the 72 h time point. We cannot exclude the possibility that other minor products such as the six-membered-ring cyclization product are present in some samples, but if present there must be less than 5%.

Catalyzed cyclization of secondary amine **26b** to give **27b** was also examined (Table 3). Catalysts **2**, **4**, and **6** all cyclized the secondary amine much more quickly than was the case for the primary amine, with pyrimidyl species **4** working slightly faster than pyridyl analogue **6**, which was in turn slightly faster than imidazolyl analogue **2**. The observed relative rate of reactivity suggests that there may be an inverse correlation between the basicity of the chelating nitrogen group and the reactivity of the catalyst for interacting with incoming proton donors; although given the significant differences in basicity between imidazole, pyridine, and pyrimidine, it would appear that hemilability rather than basicity is the dominant factor in the reactions examined.[35] Pyridyl catalyst **6** appears to give the cleanest reaction mixture.

CONCLUSIONS

Complex **1**, lacking a hindered pyridyl substituent, was known to form a chelate, which from our previous studies on fluxionality of the similar pyrimidyl analogue **3** would be tightly bound. Successful formation of a weakly N-coordinated analogue (**6**) was achieved by synthesizing a ligand with not only a *tert*-butyl group at C-6, next to the pyridyl nitrogen, but also a second *tert*-butyl group at C-4, to avoid metalation by the Cp*Ir fragment (seen in **22** and **23**). In solution, ^{15}N NMR chemical shift information on di-*tert*-butylated species **6** was consistent with the expected chelate structure, whereas slow growth of a crystal suitable for X-ray diffraction led to chloride-bridged dimer $(\mathbf{6})_2$.

Complex **6** catalyzes intramolecular hydroamination much faster than its less substituted analogue **1**, as well as faster than carbene-free precursor $[Cp^*Ir(\mu\text{-}Cl)Cl]_2$. Comparing (heteroaryl)NHC species **2**, **4**, and **6**, each with a *tert*-butyl group next to the nitrogen, which enables hydroamination, the rate differences are somewhat modest but increase in the order imidazolyl < pyridyl < pyrimidyl, which may be an effect of basicity but because of the similarity in rates is perhaps better ascribed to hemilability or counterbalancing of more than one factor. The current study highlights the need to weaken chelation by steric hindrance, as well as use a variety of techniques, particularly ^{15}N NMR spectra, to determine catalyst structure. Moreover, the new functionalized imidazolium salts **10** and **19** and NHC ligands in silver complexes **20** and **21** are expected to be useful in creating other novel bifunctional catalysts.

EXPERIMENTAL SECTION

General Methods. Reactions were performed under dry nitrogen, using a combination of Schlenk line and glovebox techniques. $CDCl_3$ was distilled from CaH_2 prior to use. NMR tube reactions were performed in resealable NMR tubes (J. Young). Unless otherwise specified, ^{1}H and ^{13}C data were measured at 30 °C on a 400 MHz spectrometer (399.8 MHz for ^{1}H and 100.5 MHz for ^{13}C) and ^{15}N data on a 600 MHz spectrometer. ^{1}H and ^{13}C NMR chemical shifts are reported in ppm downfield from tetramethylsilane and referenced to solvent resonances (^{1}H NMR: δ 7.27 for $CHCl_3$, δ 5.32 for $CHDCl_2$; ^{13}C NMR: δ 77.23 for $CDCl_3$, δ 54.00 for CD_2Cl_2). ^{1}H NMR signals are given followed by multiplicity, coupling constants J in hertz, and integration in parentheses. For complex coupling patterns, the first coupling constant listed corresponds to the first splitting listed; for example, for (dt, J = 3.2, 7.9, 1 H) the doublet exhibits a 3.2 Hz coupling constant. Raman spectra at ambient temperatures were obtained on a Thermo Scientific DXR Raman microscope with an excitation laser set at 532 nm. Samples were examined in CD_2Cl_2 solutions in quartz cells. Elemental analyses were performed at NuMega Laboratories in San Diego, CA, USA.

Synthesis of **6**. In a 20 mL screw cap vial, solid $(Cp^*Ir(\mu\text{-}Cl)Cl)_2$ (0.3309 g, 0.4183 mmol) was added to **21** (0.3304 g, 0.4153 mmol) and silver hexafluorophosphate (0.1077 g, 0.4260 mmol) in CH_2Cl_2 (1 mL) under nitrogen. The resulting mixture was stirred for 18 h. The orange-red mixture was filtered through Celite in order to remove the silver chloride; the filter cake was rinsed with CH_2Cl_2 (5 mL total) in several portions. The orange-red solution was purified by column

dx.doi.org/10.1021/om400758b | *Organometallics* 2013, 32, 6400−6409

chromatography on silica gel using ethyl acetate to elute product. The red solvent was removed using a rotary evaporator, and then the solid was placed under oil-pump vacuum for 1 day, leaving **6** as a red foam (0.4956 g, 0.6360 mmol, 77% yield). Red crystals were grown using vapor diffusion of ether into ethyl acetate for X-ray analysis, which revealed that the crystals consisted of the dimer $(\mathbf{6})_2$, whereas solution-phase ^{15}N NMR data for the single species detected by ^{1}H and ^{13}C NMR are consistent with formulation as monomeric **6**. Anal. Calcd for $C_{27}H_{40}ClF_6IrN_3P$ (779.26 g/mol): C, 41.61; H, 5.17; N, 5.39. Found: C, 41.45; H, 5.30; N, 5.39. ^{1}H NMR (CD_2Cl_2, 599.6 MHz): δ 7.73 (s, 1H), 7.64 (s, 1H), 7.47 (s, 1H), 7.33 (d, J = 2.1, 1H), 4.01 (s, 3H), 1.52 (s, 9H), 1.48 (s, 15H), 1.41 ppm (s, 9H). ^{13}C{^{1}H} NMR (CD_2Cl_2, 150.8 MHz): δ 174.9, 168.0, 166.3, 154.4, 126.1, 120.0, 119.8, 108.8, 92.9, 41.1, 37.2, 36.3, 32.4, 30.6, 9.7 ppm.

Synthesis of ***8***. In a glovebox, a 250 mL Schlenk flask with a stir bar was charged with NaH (1.658 g, 61.1 wt % in oil, 42.2 mmol) and NMP (30 mL). Outside the glovebox, the flask was placed in an ice bath. Under positive nitrogen flow imidazole (2.93 g, 43.0 mmol) was added in portions over 5 min, producing foaming, and the flask was capped with a septum once more. After 5 min, the ice bath was removed. After 50 min, under positive nitrogen flow was added 6-*tert*-butyl-2-chloropyridine (**7**, 5.71 g, 33.7 mmol; see ref 36 for synthesis of ^{15}N-labeled analogue). The flask was capped with a septum once more, and the flask was placed in a 140 °C oil bath for 44 h. To the cooled mixture was added water (150 mL), and the resulting mixture was extracted with CH_2Cl_2 (5 × 50 mL). Analysis by TLC showed that most product was in extracts 1 and 2, with a trace in 4. Extracts 1 and 2 were combined, as were 3 and 4, and each portion was washed with water (3 × 125 mL). The combined aqueous washes were back-extracted with CH_2Cl_2 extract 5. After drying, filtration, and concentration, crude product (14.5 g) was purified by flash chromatography over silica, eluting with ethyl acetate/petroleum ether (1:4) containing some aqueous ammonia. Product-containing fractions were concentrated, and the residue (6.66 g) was recrystallized from CH_2Cl_2, hexane, and pentane. **8** was afforded as colorless crystals (5.81 g, 86%). Anal. Calcd for $C_{12}H_{15}N_3$ (201.27 g/mol): C, 71.61; H, 7.51; N, 20.88. Found: C, 71.71; H, 7.17; N, 21.00. ^{1}H NMR ($CDCl_3$, 499.94 MHz): δ 8.40 (narrow m, 1H), 7.73 (t, J = 7.7, 1H), 7.67 (narrow m, 1H), 7.26 (d, J = 8, 1H), 7.19 (narrow m, 1H), 7.14 ppm (d, J = 8, 1H).

Synthesis of ***9***. Compound **8** (0.9105 g, 4.52 mmol) and iodomethane (6.940 g, 48.9 mmol) were added to a round-bottom flask with a magnetic stir bar under nitrogen. The reaction was then left to stir under nitrogen for 24 h. Excess iodomethane was then removed under vacuum. The **9** appeared as an off-white solid (1.5026 g, 4.38 mmol, 97% yield). Anal. Calcd for $C_{13}H_{18}N_3I$ (343.21 g/mol): C, 45.49; H, 5.29; N, 12.24. Found: C, 45.12; H, 5.01; N, 12.06. ^{1}H NMR ($CDCl_3$, 599.6 MHz): δ 10.99 (s, 1H), 8.26 (t, J = 1.8, 1.8, 1H), 8.07 (d, J = 7.9, 1H), 7.92 (dd, J = 8.2, 7.9, 1H), 7.71 (t, J = 1.8, 1.8, 1H), 7.46 (d, J = 7.9, 1H), 4.31 (s, 3H), 1.36 ppm (s, 9H). ^{13}C{^{1}H} NMR ($CDCl_3$, 150.8 MHz): δ 170.2, 144.5, 140.7, 135.0, 124.1, 120.8, 118.8, 111.4, 37.73, 37.68, 29.9 ppm.

Synthesis of ***10*** *(ref 37)*. Solid **9** (0.3004 g, 0.875 mmol) was added to a 20 mL vial, followed by acetone (10 mL) as the solvent. To the resulting suspension was added while stirring potassium hexafluorophosphate (0.1620 g, 0.880 mmol) dissolved in acetone (5 mL). The reaction turned a pale yellow color and was then left to stir for 2 h at room temperature. The mixture was filtered through Celite, the filter cake was rinsed with acetone (5 mL), and the combined filtrates were concentrated by rotary evaporation. In order to ensure that the ion exchange fully took place, more potassium hexafluorophosphate (0.1674 g, 0.909 mmol) dissolved in methanol (5 mL) was added while stirring. After 2 h water was added to precipitate the product as a solid, the mixture was filtered, and the solid was dried. Product **10** appeared as a pale yellow solid (0.1496 g, 0.414 mmol, 47% yield). Anal. Calcd for $C_{13}H_{18}F_6N_3P$ (361.27 g/mol): C, 43.22; H, 5.02; N, 11.63. Found: C, 43.60; H, 4.66; N, 11.90. ^{1}H NMR (CD_2Cl_2, 499.94 MHz, 20 s acquisition time giving digital resolution of 0.05 Hz per point): δ 9.28 (narrow m, 1H), 8.13 (t, J = 1.9, 1H), 7.97 (t, J = 8.0, 1H), 7.56 (dd, J = 0.5, 8.0, 1H), 7.54 (d, J = 8.0, 1H), 7.48 (t, J = 1.8, 1H), 4.10 (s, 3H), 1.41 ppm (s, 9H). ^{13}C{^{1}H} NMR (CD_2Cl_2, 150.8 MHz): δ 171.3, 145.2, 141.3, 134.2, 124.9, 121.8, 120.0, 110.8, 38.3, 37.7, 30.2 ppm.

Synthesis of ***12***. A heat-dried 200 mL flask, under nitrogen in the glovebox, was charged with triethylamine (100 mL). Pivaloyl chloride (8.606 g, 71.4 mmol) was then added to the flask, forming a white solid. 3,3-Dimethylbut-1-yne (5.860 g, 71.3 mmol) was added, followed by palladium dichloride bis-triphenylphosphine (0.050 g, 0.071 mmol) and copper iodide (0.198 g, 1.04 mmol). The yellow solution was stirred at 23 °C for 1.5 h, at which point the solution turned a green color. The reaction was then stirred for an additional 18.5 h, and an aliquot for ^{1}H NMR was taken to check the reaction. Starting material was still observed, so an additional portion of palladium dichloride bis-triphenylphosphine (0.050 g, 0.071 mmol) was added to the reaction. After 4 h the starting material was no longer observed by ^{1}H NMR, and the reaction was worked up using water (200 mL) and diethyl ether (500 mL). The resulting heterogeneous mixture was extracted with diethyl ether (3 × 200 mL) in a 1000 mL separatory funnel. The first three organic extracts were combined and washed with 1 M HCl (200 mL). The diethyl ether layer was then washed with a saturated solution of sodium bicarbonate (50 mL) followed by a saturated solution of ammonium chloride (50 mL). Organic extracts were dried over $MgSO_4$ and filtered, and the filtrate was concentrated. The sample was then purified through partial vacuum distillation. Using a distillation setup with a fractionating column and an oil bath, the oil bath was heated to 110 °C and the pressure was slowly reduced to 25 mmHg. Pure product was collected at 82−86 °C, resulting in **12** as a slightly yellow oil (9.6278 g, 57.9 mmol, 81%). NMR data matched literature values.[21]

Synthesis of ***13***. Compound **13** was made following the procedure as reported in the literature.[21] NMR data matched literature values for the product. ^{1}H NMR ($CDCl_3$, 399.76 MHz): δ 6.11 (s, 1H), 3.89 (s, 3H), 1.29 (s, 9H), 1.28 (s, 9H). However, an impurity was also observed every time the reaction was run. ^{1}H NMR (may be partial) ($CDCl_3$, 399.76 MHz): δ 5.71 (s, 1H), 3.78 (s, 3H), 3.62 (s, 1H), 1.17 (s, 9H), 1.14 ppm (s, 9H).

Synthesis of ***14*** *and* ***15***. Two thick-walled pressure reaction tubes (48 mL volume each) were charged with half of a sample of **13** (containing ca. 15% of unknown impurity from its reported synthesis) (2.833 g, 10.6 mmol assuming 100% purity). To each tube was added 1,4-dioxane (6 mL) followed by concentrated ammonium hydroxide (12 mL to each). Each tube was sealed with a threaded Teflon stopper, and the tubes were heated for 2.8 h in an oil bath held at 80 °C, behind a safety shield, as the contents were stirred. Initially, within about 20 min the solids mostly dissolved, giving a cloudy mixture. After an additional 15 min and thereafter, reappearance of solids was noted. After a total of 2.8 h, the tubes were allowed to cool before the contents were transferred to a round-bottom flask. Methanol was used in portions for quantitative transfer. The mixture was concentrated to dryness by rotary evaporation, followed by storage under oil pump vacuum overnight, leaving a white solid (2.23 g). Analysis by ^{1}H, ^{13}C{^{1}H}, HSQC, and HMBC NMR spectroscopy was consistent with the presence of **14** and **15**, in a molar ratio of 1 to 10. For **15** in the mixture: ^{1}H NMR ($CDCl_3$, 499.94 MHz): δ 10.94 (br s, 1H), 6.36 (d, J = 1.5, 1H), 6.13 (d, J = 1.5, 1H), 1.36 (s, 9H), 1.25 ppm (s, 9H). ^{13}C{^{1}H} NMR ($CDCl_3$, 125.72 MHz): δ 165.53, 165.37, 112.8, 100.5, 35.50, 35.09, 30.2, 29.3 ppm.

For the intermediate **14** (tentatively identified) in the mixture: ^{1}H ($CDCl_3$, 499.94 MHz): δ 12.00 (br s, 1H), 6.18 (s, 1H), 3.87 (s, 3H), 1.32 (s, 9H); second *t*-Bu singlet obscured by large singlet for carbocyclic group at 1.36 ppm. ^{13}C{^{1}H} NMR ($CDCl_3$, 125.72 MHz): δ 169.6, 163.5, 160.2, 156.0, 100.8, 52.3, 36.8, 35.3, 30.5, 29.2 ppm.

To the solid was added concentrated sulfuric acid (12 mL), and the resulting syrup was stirred as the flask was held in a 100 °C oil bath for 2 h. The flask was cooled in ice, and ice chips (ca. 50 cm^3) were added, followed by portions of KOH (20.0 g) in water (15 mL). The mixture was still acidic (pH = 1), but by adding portionwise most of a mixture of K_2CO_3 (20.3 g) and water (20 mL) until no more foaming was evident, the pH was raised to 9. The resulting heterogeneous mixture was diluted with water (200 mL) and extracted with CH_2Cl_2 (1 × 100

dx.doi.org/10.1021/om400758b | *Organometallics* 2013, 32, 6400−6409

mL, 3 × 50 mL) in a 250 mL separatory funnel. The first three organic extracts were combined and washed with water (2 × 100 mL). The two water washes were combined and back-extracted with the fourth CH_2Cl_2 extract. Organic extracts were dried over $MgSO_4$ and filtered, and the filtrate was concentrated. The white solid was stored under an oil pump vacuum for 1 d, leaving **15** (1.94 g, 9.35 mmol, 88% overall yield from **13**). Anal. Calcd for $C_{13}H_{21}NO$ (207.32 g/mol): C, 75.32; H, 10.21; N, 6.76. Found: C, 76.31; H, 10.91; N, 7.14. ^{1}H NMR ($CDCl_3$, 599.6 MHz): δ 10.94 (s, 1H), 6.36 (s, 1H), 6.13 (s, 1H), 1.36 (s, 9H), 1.25 ppm (s, 9H). $^{13}C\{^1H\}$ NMR ($CDCl_3$, 150.8 MHz): δ 165.5, 165.4, 155.3, 112.8, 100.5, 35.5, 35.1, 30.2, 29.3 ppm.

Synthesis of ***16***. Compound **15** (2.47 g, 11.9 mmol) was added to a dry 100 mL Schlenk flask containing phosphorus oxychloride (2.1 mL) as the solvent. The solution was then bubbled with nitrogen gas for 5 min, and the flask was placed in a 100 °C oil bath. Phosphorus pentachloride (2.853 g, 13.7 mmol) was then added to the reaction slowly, with fizzing seen while stirring, while kept under a nitrogen atmosphere. A condenser was then attached to the flask, and the oil bath was heated to 165 °C. After 1 h the reflux was stopped, and the volatiles were removed under reduced pressure (20 mmHg) at 120 °C. The residue was a white solid with a yellow-colored oil. To this was added water (24 mL), and the reaction was set in an ice bath. Potassium hydroxide (3.8966 g, 68.5 mmol) was slowly added to the flask to adjust the pH. The yellow-colored solution was then worked up using water (5 mL) and diethyl ether (50 mL) in a 250 mL separatory funnel. The aqueous layer was then extracted four times with diethyl ether (4 × 25 mL). The organic layers were then combined and washed with two portions of saturated potassium carbonate solution (2 × 40 mL) and once with water (40 mL). The organic layer was dried over magnesium sulfate, and most of the yellow colorant was removed on a plug of silica, using diethyl ether as the solvent. The solvent was removed under vacuum to give **16** as a pale yellow oil (2.3458 g, 10.4 mmol, 89% yield). Anal. Calcd for $C_{13}H_{20}ClN$ (225.76 g/mol): C, 69.16; H, 8.93; N, 6.20. Found: C, 68.90; H, 9.32; N, 6.47. ^{1}H NMR ($CDCl_3$, 599.6 MHz): δ 7.21 (s, 1H), 7.10 (s, 1H), 1.36 (s, 9H), 1.31 ppm (s, 9H). $^{13}C\{^1H\}$ NMR ($CDCl_3$, 150.8 MHz): δ 170.2, 163.4, 150.5, 108.2, 114.5, 37.6, 35.1, 30.6, 30.1 ppm.

Synthesis of ***17***. On the balance, **16** (0.148 g, 0.656 mmol) was added to a dry 25 mL flask; then dimethyl sulfoxide (1.3 mL) was added as the solvent. Imidazole (0.0672 g, 0.984 mmol), copper(I) iodide (0.0272 g, 0.0656 mmol), and potassium hydroxide (0.0789 g, 1.41 mmol) were then added to the reaction flask in that order. The solution, green in color, was then bubbled with nitrogen gas for 5 min, and the flask placed in a 150 °C oil bath for 48 h. After 1 h of heating the reaction solution turned a dark red color. The reaction was checked periodically by analyzing aliquots by ^{1}H NMR spectroscopy until all of the peaks for the starting material were gone. The red liquid was then worked up with 10 mL of 10% ammonium hydroxide and 30 mL of methylene chloride in a 150 mL separatory funnel. The brown-colored aqueous phase was then extracted with three portions of CH_2Cl_2 (3 × 20 mL). The organic layers were then combined and washed with 10 mL of saturated ammonium chloride solution. The organic layer, a brown color, was dried over sodium sulfate, and most of the brown colorant was removed by passing the mixture through a plug of silica, using CH_2Cl_2 as the eluant. After concentration, the residue was further purified through recrystallization using the diffusion of pentane into a diethyl ether solution while the sample was kept in the freezer. Product **17** appeared as a white crystalline solid (0.797 g, 0.380 mmol, 47% yield). Anal. Calcd for $C_{16}H_{23}N_3$ (257.37 g/mol): C, 74.67; H, 9.01; N, 16.33. Found: C, 74.47; H, 8.95; N, 16.09. ^{1}H NMR ($CDCl_3$, 599.6 MHz): δ 8.38 (s, 1H), 7.68 (s, 1H), 7.26 (d, J = 1.6, 1H), 7.19 (s, 1H), 7.11 (d, J = 1.6, 1H), 1.39 (s, 9H), 1.37 ppm (s, 9H). $^{13}C\{^1H\}$ NMR ($CDCl_3$, 150.8 MHz): δ 169.2, 163.7, 148.1, 135.1, 130.3, 116.2, 114.2, 106.0, 37.7, 35.3, 30.7, 30.1 ppm.

Synthesis of ***18***. To solid **17** (0.2780 g, 1.08 mmol) in a vial was added iodomethane (1.940 g, 13.7 mmol), and the resulting mixture was stirred for 0.5 h. The mixture was concentrated on the rotary evaporator. Analysis of the crude product by NMR spectroscopy showed about 10% unreacted **17**. Thus, iodomethane (0.90 g, 6.3 mmol) was added, and the mixture was stirred for 1 h. A third treatment with iodomethane (0.61 g, 4.3 mmol) for 21 h afforded product **18** as white solid (0.4366 g, 1.09 mmol, 101% yield), suitable for the next step. A sample from another smaller reaction was isolated in 94% yield and gave correct analytical data. Anal. Calcd for $C_{17}H_{26}IN_3$ (399.31 g/mol): C, 51.13; H, 6.56; N, 10.52. Found: C, 50.90; H, 6.39; N, 10.66. ^{1}H NMR ($CDCl_3$, 499.94 MHz): δ 11.62 (s, 1H), 8.23 (dd, J = 2.0, 1.7, 1H), 8.12 (d, J = 1.2, 1H), 7.47 (d, J = 1.2, 1H), 7.32 (dd, J = 1.7, 1.7, 1H), 4.30 (s, 3H), 1.46 (s, 9H), 1.40 ppm (s, 9H).

Synthesis of ***19***. Compound **18** (0.1266 g, 0.317 mmol) was added to a 20 mL vial with acetone (2 mL) as the solvent. To this was added, while stirring, potassium hexafluorophosphate (0.0613 g, 0.333 mmol) dissolved in water (2 mL). The reaction turned a pale yellow color and was then left to stir for 1 h at room temperature. The acetone was then removed under vacuum, and a white solid precipitated out of the solution. An aqueous workup was done using 5 mL of water and 5 mL of CH_2Cl_2 in a 60 mL separatory funnel. The aqueous phase was then extracted with three portions of CH_2Cl_2 (3 × 5 mL). The organic layers were then combined, and the CH_2Cl_2 was removed under vacuum. Product **19** appeared as a white solid (0.114 g, 0.273 mmol, 86% yield). Anal. Calcd for $C_{17}H_{26}F_6N_3P$ (417.37 g/mol): C, 48.92; H, 6.28; N, 10.07. Found: C, 49.20; H, 6.06; N, 10.33. ^{1}H NMR ($CDCl_3$, 599.6 MHz): δ 9.35 (s, 1H), 8.17 (d, J = 1.8, 1H), 7.57 (s, 1H), 7.50 (d, J = 1.8, 1H), 7.45 (s, 1H), 4.10 (s, 1H), 1.37 (s, 9H), 1.36 ppm (s, 9H). $^{13}C\{^1H\}$ NMR ($CDCl_3$, 150.8 MHz): δ 170.0, 166.0, 145.0, 133.8, 124.1, 119.4, 117.6, 108.0, 37.8, 36.8, 35.7, 30.4, 30.0 ppm.

Synthesis of ***20***. In the glovebox, a scintillation vial was charged with solid **10** (0.1014 g, 0.281 mmol) and silver oxide (0.0281 g, 0.121 mmol). To the solids were added a stir bar, CH_2Cl_2 (4 mL), followed by aqueous NaOH (0.28 mL, 1 M). The resulting mixture was stirred. Analysis of an aliquot (ca. 0.5 mL) with CD_2Cl_2 added for NMR lock showed clean conversion. Outside the glovebox, the vial and aliquot NMR tube contents were transferred quantitatively to a separatory funnel using CH_2Cl_2 (5 mL in portions) and water (5 mL). The aqueous phase was extracted with two portions of CH_2Cl_2 (2 × 5 mL). The combined organic phases were washed with water (5 mL), and the methylene chloride was removed under vacuum (no drying agent used). The residue was taken up in CH_2Cl_2 (ca. 2 mL) and filtered through a 0.2 μm syringe filter into a tared vial, and the solution concentrated. The solids were taken up in CH_2Cl_2 (1 mL), and pentane was added in portions to precipitate the product. After a few minutes, the pale yellow supernatant was pipetted off carefully, leaving a white solid, which was dried in air in the dark, then under oil pump vacuum for 1 h. Yield of **20** as a white powder: 0.0965 g, 100.6%. Some of this sample was used for an experiment, leaving 55.7 mg, which was stored under oil pump vacuum for an additional 35 h, affording 53.8 mg, part of which was used to obtain combustion analysis; thus the yield of **20** was 97%. Anal. Calcd for $C_{26}H_{34}AgF_6N_6P$ (683.42 g/mol): C, 45.69; H, 5.01; N, 12.30. Found: C, 45.68; H, 4.84; N, 12.43. ^{1}H NMR (CD_2Cl_2, 599.6 MHz): δ 7.78 (d, J = 2.0, 1H), 7.76 (t, J = 7.9, 1H), 7.54 (dd, J = 0.7, 7.9, 1H), 7.40 (dd, J = 0.5, 7.9, 1H), 7.29 (d, J = 2.0, 1H), 3.98 (s, 3H), 1.26 ppm (s, 9H). $^{13}C\{^1H\}$ NMR (CD_2Cl_2, 150.8 MHz): δ 181.2 (looks like br d, $J \approx 195$), 170.4, 150.3, 140.1, 123.8 (d, J = 5.1), 121.0 (d, J = 4), 119.8, 112.6, 40.2, 38.0, 30.3 ppm.

Synthesis of ***21***. Solid **19** (0.0474 g, 0.114 mmol) was added to a 20 mL vial, wrapped in foil to keep light out, followed by CH_2Cl_2 (2 mL) as the solvent. To the resulting solution was added sodium hydroxide (0.1 mL, 1 M) followed by silver oxide (0.0096 g, 0.041 mmol). The mixture was set to stir under nitrogen for 22 h. The resulting mixture was a tan color solution. An aqueous workup was done using 5 mL of water and 5 mL of CH_2Cl_2 in a 60 mL separatory funnel. The aqueous phase was then extracted with three portions of CH_2Cl_2 (2 × 5 mL). The organic layers were then combined, and the CH_2Cl_2 was removed under vacuum. Product **21** appeared as a tan foam (0.0440 g, 0.0553 mmol, 97% yield). Anal. Calcd for $C_{34}H_{50}AgF_6N_6P$ (795.63 g/mol): C, 51.33; H, 6.33; N, 10.56. Found: C, 51.60; H, 6.23; N, 10.66. ^{1}H NMR (CD_2Cl_2, 599.6 MHz): δ 7.80 (t, J = 1.6, 2H), 7.52 (d, J = 1.3, 2H),

dx.doi.org/10.1021/om400758b | *Organometallics* 2013, 32, 6400−6409

7.35 (d, J = 1.3, 2H), 7.30 (t, J = 1.6, 2H), 4.00 (s, 6H), 1.25 (s, 18H), 1.20 ppm (s, 18H). $^{13}C\{^1H\}$ NMR (CD_2Cl_2, 150.8 MHz): δ 181.2 (two d, $^1J_{C-Ag-109}$ = 214.9, $^1J_{C-Ag-107}$ = 185.7), 170.0, 164.8, 150.6, 123.7 (d, J = 5.6), 121.0 (d, J = 5.0), 116.7, 109.7, 40.2, 38.1, 35.8, 30.8, 30.4 ppm.

Attempted Synthesis of ***5****, Forming* ***22*** *and Then* ***23****.* In a 20 mL screw cap vial, solid $(Cp^*Ir(\mu\text{-}Cl)Cl)_2$ (0.0547 g, 0.0676 mmol) was added to **20** (0.0462 g, 0.0676 mmol) and silver hexafluorophosphate (0.0170 g, 0.0676 mmol) in CH_2Cl_2 (1 mL) under nitrogen. The resulting mixture was stirred for 12 h. The orange-red mixture was filtered through Celite in order to remove the silver chloride; the filter cake was rinsed with CH_2Cl_2 (5 mL total) in several portions. An aliquot of the orange-yellow-colored solution was checked by ^1H NMR spectroscopy in CD_2Cl_2, and a spectrum consistent with compound **22** was observed, indicated by a broad peak at 12.63 ppm, ascribed to a protonated pyridine nitrogen NH, and only two sharp doublets for pyridine ring protons at 8.54 and 7.26 ppm (J = 7.6 Hz); this pattern was nothing like the three separate signals (two doublets and a triplet) expected around 7 to 8 ppm for the three-spin system of the pyridine ring protons shown in **5**. The proton was then removed from the pyridine nitrogen by dissolving the solid in CH_2Cl_2 and adding Amberjet 4400 OH resin (0.092 g), then swirling the solution for approximately 5 min. The solution turned a deep red color. The Amberjet was then removed by passing the sample through a Celite filter using 5 mL of CH_2Cl_2 in small portions. The CH_2Cl_2 was then removed using a rotary evaporator, and then the solid was set to recrystallize by dissolving the sample in toluene and slowly diffusing hexanes while in the freezer. The crystals were then set to dry under vacuum for 1 day, leaving **23** as a red solid (0.0388 g, 0.0537 mmol, 40% yield). Red crystals were then grown using vapor diffusion of ether into ethyl acetate for X-ray analysis. The X-ray analysis and elemental analysis were done using samples made in previous experiments that had lower yields. Anal. Calcd for $C_{23}H_{31}ClIrN_3$ (577.18 g/mol): C, 47.86; H, 5.41; N, 7.28. Found: C, 48.22; H, 5.80; N, 7.05. ^1H NMR ($CDCl_3$, 599.5 MHz): δ 7.93 (d, J = 7.7, 1H), 7.64 (s, 1H), 6.97 (s, 1H), 6.93 (d, J = 7.7, 1H), 3.98 (s, 3H), 1.81 (s, 15H), 1.35 ppm (s, 9H). $^{13}C\{^1H\}$ NMR ($CDCl_3$, 150.76 MHz): δ 162.8, 161.1, 159.2, 143.7, 130.3, 121.1, 116.6, 115.7, 90.6, 36.56, 36.40, 30.4, 9.7 ppm.

X-ray Crystallography. All crystallographic data were collected on Bruker diffractometers equipped with APEX CCD detectors. All structures were solved by direct methods and refined with anisotropic thermal parameters and idealized hydrogen atoms. All software is contained in the SMART, SAINT, and SHEXTL libraries distributed by Bruker-AXS (Madison, WI, USA). Complete disclosures about the crystallographic work may be found in the deposited CIF file.

Hydroamination. For the cyclization studies, using either primary or secondary amine compounds the methodology for testing was similar. Either 2,2-dimethylpent-4-en-1-amine as the primary amine or *N*,2,2-trimethylpent-4-en-1-amine as the secondary amine (0.25 mmol) and catalyst (5 mol %; 2.5 mol % in the case of $[Cp^*Ir(\mu\text{-}Cl)Cl]_2$ in THF-d_8 (1.0 mL) were used at 100 °C. Yields shown are based on ^1H NMR spectroscopy, averaging results from two separate runs, except for $[Cp^*Ir(\mu\text{-}Cl)Cl]_2$, using 1,3,5-trimethoxybenzene as an internal standard.

■ ASSOCIATED CONTENT

Supporting Information

Additional figures including graphical summaries of 2D NMR data and assignments of all proton and carbon resonances for compounds **6**, **9**, **10**, **14**−**17**, **19**−**21**, and **23**, Raman spectra and analysis, and CIF files for complexes **6** and **23**. This material is available free of charge via the Internet at http://pubs.acs.org.

■ AUTHOR INFORMATION

Corresponding Author

*E-mail: grotjahn@chemistry.sdsu.edu. Fax: (+1) 619-594-4634. Tel: (+1) 619-594-0231.

Notes

The authors declare no competing financial interest.

■ ACKNOWLEDGMENTS

We thank the San Diego Foundation, SDSU, and NSF for partial support of this work, including SDSU NMR facilities (MRI CHE-0521698).

■ REFERENCES

(1) Kantchev, E. A. B.; O'Brien, C. J.; Organ, M. G. *Angew. Chem., Int. Ed.* **2007**, *46*, 2768−2813.
(2) Vougioukalakis, G. C.; Grubbs, R. H. *Chem. Rev.* **2010**, *110*, 1746−1787.
(3) Diez-Gonzalez, S.; Marion, N.; Nolan, S. P. *Chem. Rev.* **2009**, *109*, 3612−3676.
(4) Strassner, T. *Topics in Organometallic Chemistry* **2007**, *22*, 125−148.
(5) Diez-Gonzalez, S.; Nolan, S. P. *Coord. Chem. Rev.* **2007**, *251*, 874−883.
(6) Crabtree, R. H. *J. Organomet. Chem.* **2005**, *690*, 5451−5457.
(7) Hahn, F. E.; Jahnke, M. C. *Angew. Chem., Int. Ed.* **2008**, *47*, 3122−3172.
(8) Scott, N. M.; Nolan, S. P. *Eur. J. Inorg. Chem.* **2005**, 1815−1828.
(9) Herrmann, W. A. *Angew. Chem., Int. Ed. Engl.* **2002**, *41*, 1290−1309.
(10) Weskamp, T.; Bohm, V. P. W.; Herrmann, W. A. *J. Organomet. Chem.* **2000**, *600*, 12−22.
(11) Bourissou, D.; Guerret, O.; Gabbaie, F. P.; Bertrand, G. *Chem. Rev.* **2000**, *100*, 39−91.
(12) Specht, Z. G.; Cortes-Llamas, S. A.; Tran, H. N.; Niekerk, C. v.; Rancudo, K. T.; Golen, J. A.; Moore, C. E.; DiPasquale, A. G.; Rheingold, A. L.; Dwyer, T. J.; Grotjahn, D. B. *Chem.—Eur. J.* **2011**, *17*, 6606−6609.
(13) Smith, D. L.; Elving, P. J. *J. Am. Chem. Soc.* **1962**, *84*, 2741−2747.
(14) Krygowski, T. M.; Szatylowicz, H.; Zachara, J. E. *J. Org. Chem.* **2005**, *70*, 8859−8865.
(15) Xiao, X.-Q.; Jin, G.-X. *J. Organomet. Chem.* **2008**, *693*, 3363−3368.
(16) Gnanamgari, D.; Sauer, E. L. O.; Schley, N. D.; Butler, C.; Incarvito, C. D.; Crabtree, R. H. *Organometallics* **2009**, *28*, 321−325.
(17) Mas-Marza, E.; Sanau, M.; Peris, E. *J. Organomet. Chem.* **2005**, *690*, 5576−5580.
(18) Peng, H. M.; Webster, R. D.; Li, X. *Organometallics* **2008**, *27*, 4484−4493.
(19) Sun, J.-F.; Chen, F.; Dougan, B. A.; Xu, H.-J.; Cheng, Y.; Li, Y.-Z.; Chen, X.-T.; Xue, Z.-L. *J. Organomet. Chem.* **2009**, *694*, 2096−2105.
(20) Grotjahn, D. B.; Van, S.; Combs, D.; Lev, D.; Schneider, C.; Rideout, M.; Meyer, C.; Hernandez, G.; Mejorado, L. *J. Org. Chem.* **2002**, *67*, 9200−9209.
(21) Miller, M. J.; Lyttle, M. H.; Streitwieser, A., Jr. *J. Org. Chem.* **1981**, *46*, 1977−1984.
(22) Wang, H. M. J.; Lin, I. J. B. *Organometallics* **1998**, *17*, 972−975.
(23) Arduengo, A. J., III; Dias, H. V. R.; Calabrese, J. C.; Davidson, F. *Organometallics* **1993**, *12*, 3405−3409.
(24) Bildstein, B.; Malaun, M.; Kopacka, H.; Wurst, K.; Mitterboeck, M.; Ongania, K.-H.; Opromolla, G.; Zanello, P. *Organometallics* **1999**, *18*, 4325−4336.
(25) De Fremont, P.; Scott, N. M.; Stevens, E. D.; Ramnial, T.; Lightbody, O. C.; Macdonald, C. L. B.; Clyburne, J. A. C.; Abernethy, C. D.; Nolan, S. P. *Organometallics* **2005**, *24*, 6301−6309.

(26) Li, L.; Brennessel, W. W.; Jones, W. D. *J. Am. Chem. Soc.* **2008**, *130*, 12414−12419.
(27) Maitlis, P. M.; White, C.; Gill, D. S.; Kang, J. W.; Lee, H. B. *J. Chem. Soc. D, Chem. Commun.* **1971**, 734−735.
(28) White, C.; Oliver, A. J.; Maitlis, P. M. *J. Chem. Soc., Dalton Trans.* **1973**, 1901−1907.
(29) Gill, D. S.; Maitlis, P. M. *J. Organomet. Chem.* **1975**, *87*, 359−364.
(30) Nakamoto, K. *Infrared and Raman Spectra of Inorganic and Coodination Compounds, Part B, sixth ed.*; Wiley: Hoboken, NJ, USA; 2009, pages 197 and 285.
(31) Grotjahn, D. B. *Dalton Trans.* **2008**, 6497−6508.
(32) Grotjahn, D. B.; Kraus, J. E.; Amouri, H.; Rager, M.-N.; Cortes-Llamas, S. A.; Mallari, A. A.; DiPasquale, A. G.; Liable-Sands, L. M.; Golen, J. A.; Zakharov, L. N.; Moore, C.; Rheingold, A. L. *J. Am. Chem. Soc.* **2010**, *132*, 7919−7934.
(33) Grotjahn, D. B. *Pure Appl. Chem.* **2010**, *82*, 635−647.
(34) Miranda-Soto, V.; Grotjahn, D. B.; Cooksy, A. L.; Golen, J. A.; Moore, C. E.; Rheingold, A. L. *Angew. Chem., Int. Ed.* **2011**, *50*, 631−635.
(35) Many mechanistic studies of hydroamination and in particular, intramolecular hydroamination have been published; for just three recent examples, please see references 35a-35c. Given the complexity of the reaction and the relatively modest effects of heterocycle on the reactions summarized in Tables 2 and 3, it is difficult to ascribe differences to any one factor. (a) Hesp, K. D.; Tobisch, S.; Stradiotto, M. *J. Am. Chem. Soc.* **2010**, *132*, 413−426. (b) Kashiwame, Y.; Kuwata, S.; Ikariya, T. *Organometallics* **2012**, *31*, 8444−8455. (c) Tobisch, S. *Chem.—Eur. J.* **2012**, *18*, 7248−7262.
(36) Grotjahn, D. B.; Kragulj, E. J.; Zeinalipour-Yazdi, C. D.; Miranda-Soto, V.; Lev, D. A.; Cooksy, A. L. *J. Am. Chem. Soc.* **2008**, *130*, 10860−10861.
(37) We thank Dr. Sara Cortes-Llamas for performing this particular experiment.